

Multiasperity Fault Model and the Nature of Short-Period Subsources

A. A. GUSEV¹

Abstract—We suggest to consider the breaking of an asperity, *i.e.*, a small contact patch between fault walls, as a typical subsorce producing an elementary short-period radiation pulse from a source of a large earthquake. Based on the results of DAS and KOSTROV we propose formulas to describe amplitudes and spectra of acceleration for a multiasperity fault/source model. The stress drop over an asperity is determined in several ways; the estimates agree to give the average value of several hundred bar. Theoretical acceleration spectral shapes for the case of similar asperities agree with the observed ones, they reproduce such features as lower-frequency f^1 slope, peak, and high-frequency cutoff. The statistical stress-drop distribution over the population of asperities, and also the related distribution of peak accelerations are discussed. These distributions are found to be the power-law ones with exponent near to 2. This means that acceleration peaks are formed normally by breaking of individual asperities. We consider small earthquakes as produced by breaking of single asperities, this idea explains the observed correlation between the upper cutoff frequency of acceleration spectrum and the typical characteristic frequency of small earthquakes.

Key words: Earthquake source spectrum, asperity, strong ground motion.

1. Introduction

To study the mechanism of short-period (SP) seismic wave generation is interesting from the general point of view of earthquake source mechanics and is also important for improved prediction of destructive ground motions. The nature of short-period wave radiation is not fully understood at present, after many years of study (*e.g.*, HOUSNER, 1955; HASKELL, 1966; SHEBALIN, 1971). The barrier model of DAS and AKI (1977) in its more definite form (AKI, 1979) and several related models (*e.g.*, BOATWRIGHT, 1982; PAPAGEORGIOU and AKI, 1983) assume that SP radiation does not simply accompany the long-period source movement and radiation but is generated by a multitude of nonoverlapping small crack-type subsources isolated from each other by strong barriers. The long-period radiation is produced due to nonrandom phasing of these subsources.

¹ Institute of Volcanology, Petropavlovsk-Kamchatsky, 683006, USSR.

This model is not completely acceptable from the tectonophysical point of view: as geological time goes, slip along a fault normally cumulates, so the supposed barriers are to be broken in a certain unclear way. From the point of view of radiation properties, the idea of nonoverlapping subsources is also somewhat dubious (GUSEV, 1983). A critical discussion of this problem from another point of view is given in BOATWRIGHT (1987). These problems made us to formulate our previous statistical model (GUSEV, 1981, 1983) as a purely descriptive one, since the nature of subsurface was not fixed there (but was discussed in some detail). The subsurface spectral shape proposed by GUSEV (1983) implicitly assumed however a crack-type subsurface.

Another way to represent a stochastic source is to introduce some random field of strength, and/or of initial stress (NUR, 1978; ANDREWS, 1980). An important result in this respect was obtained through numerical simulation by MIKUMO and MIYATAKE (1978) who showed that the distribution of strength of fault elements should be "heavy-tailed" to produce more or less realistic rupture histories.

Below we shall discuss the consequences of our assumption (GUSEV, 1986) that the typical subsurface in an earthquake source can be represented mechanically as the failure of asperity. A similar idea was proposed also by BOATWRIGHT (1987). Breaking of a single asperity on a stress-free infinite fault was studied by DAS and KOSTROV (1983). In DAS and KOSTROV (1986) these results were generalized to the case of an asperity in the center of a circular crack. Hereinafter these two papers will be referred to as DK83 and DK86. Note that the model presented here has no immediate relation to the asperity model of LAY *et al.* (1982), where a much larger object is considered as an asperity, and this object is not directly related to the generation of high-frequency waves. This object can represent however, a group of high-strength asperities of the kind discussed here. For clarity we shall speak below about a multiasperity model, which is conceptually close to the "asperity model" from the Introduction of DK83 and to the "composite asperity model" of BOATWRIGHT (1987). Several important points below are related to ideas of HANKS and JOHNSON (1976) and MCGARR (1981), who were the first to realize the close relation between individual asperities (or stress concentrations) on the fault and the properties of SP radiation.

2. Breaking of a Single Asperity and Parameters of Related Radiation

In the following section we shall introduce the notion of asperity and shall give a number of formulas describing its radiation following largely DK83 and DK86. But at first let us find out why it seems necessary to discuss asperities on nonflat fault surfaces.

At the source depth of a shallow-focus earthquake elastic deformation produced by hydrostatic (*i.e.*, lithostatic) load ("compression") is below 1%. It is known that

if there is a thin oblate spheroidal cavity in an unloaded elastic medium of aspect ratio α such that $\alpha \ll 1$, this cavity will be closed by hydrostatic load at a compression value close to α . The geological fault can be considered as a contact of uneven surfaces with some typical mismatch angle β . Extrapolating the results for a spheroidal cavity it is likely that faults with $\beta > 0.01$ keep their walls unclosed down to depths of 50–100 km. The value $\beta = 0.01$ (radian) or 0.6° , should be compared with the typical angles of deviation of actual fault surface from mean flat surface (*i.e.*, the typical slope of the surface), which are $1\text{--}2^\circ$ or greater. Therefore one can expect that the intimate contact of fault walls takes place not only on a small part of the fault surface. This is reasonable not only at depths of several km (DK83), but for shallow-focus earthquakes in general. One can suppose naturally that contact is realized in isolated, more or less isometric patches-asperities, outside of which the fault strength is zero (if the filler is fluid) or low (if the filler is plastic gouge).

The fraction of a fault surface covered with strong patches is a very important parameter in the presented theory, we shall name it the filling factor k_f . Bracketing of this parameter is one of the goals of the paper. One can say *a priori*, however, that high values of k_f as 0.3 or greater would make the whole idea of isolated strong asperities more or less senseless, so only values of k_f below 0.3 are compatible with our concept of a seismogenic fault.

As noted in DK83, shear breaking of an asperity should be the usual phenomenon when fault walls slip and can be directly relevant to the earthquake source process. Because of relative isolation, the details of breaking of each asperity weakly depend on breaking of other asperities. This enables us to begin with the breaking of a single asperity.

In DK83, the asperity is modelled as a welded circular patch between two half-spaces with free boundaries and an infinitesimally narrow crack/fault between them. The asperity is loaded by pure shear relative displacement of the half-spaces, with the given value of displacement at infinity. Breaking of this asperity produces body waves (P and S) radiated into the half-spaces. For P and SH -waves (SH being defined as polarized parallel to the fault) the waveforms are unipolar velocity pulses (displacement steps) (see Figure 1). The pulse duration (step rise time) T_a is approximately equal to the breaking time. The pulse area (step amplitude) is proportional to the integral "seismic force of asperity"

$$F_0 = \int_{\Sigma} \Delta\sigma(x,y) dS = \Delta\tau S_a \quad (1)$$

where $\Delta\sigma$ is the stress drop at a point (x,y) of asperity; Σ is the asperity surface, with area S_a and element dS , and $\Delta\tau$ is the average $\Delta\sigma$ over asperity. Note that F_0 is independent of the final slip B at the asperity. Neglecting the details of fracturing and the Doppler effect, one can introduce the variable seismic force of a point asperity $F_0(t)$ so that $F_0(0) = 0$, $F_0(T_a) = F_0(\infty) = F_0$. The far-field displacement u

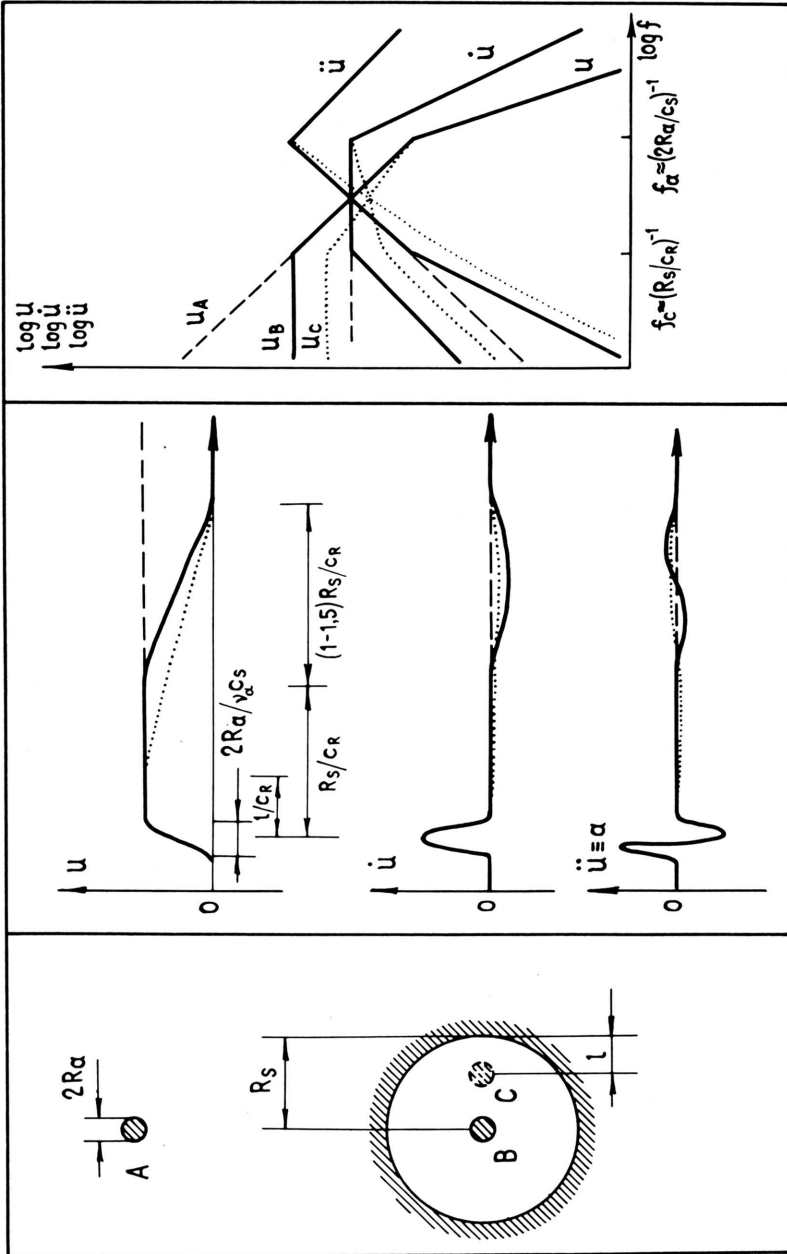


Figure 1
 Schematic view of asperity (left), body wave forms produced by its fracture (center) and their amplitude spectra (right). For cases A (two half-spaces welded over the circle-asperity), B (asperity is in the center of a circular crack, the basic case) and C (same as in B but asperity is at the boundary of the crack). Time functions and spectra are plotted by the dashed line for case A, by the solid line for case B and by the dot line for case C.

of P and SH waves is then given by the formula (replace $F_0(\cdot)$ by $\dot{F}_0(\cdot)$ or $\ddot{F}_0(\cdot)$ to obtain velocity \dot{u} or acceleration \ddot{u}):

$$u^{P,SH}(\mathbf{r},t) = \frac{D^{P,SH}F_0(t-r/c_{P,S})}{4\pi\rho c_{P,S}^2r} \quad (2)$$

where \mathbf{r} is the vector from the source to receiver, $r = |\mathbf{r}|$, ρ is the density, $c_{P,S}$ is P or S wave velocity, $D^{P,SH}$ is radiation pattern (see DK83 for details). Note that $D^{P,SH}$ can be represented as $D^{P,SH} = D_*^{P,SH}\mathcal{R}^{P,SH}$ where $\mathcal{R}^{P,SH}$ is the standard radiation pattern for a dislocation source on Σ with normal \mathbf{n} and slip direction \mathbf{b} , "along" Δt (i.e., $b_i \propto n_j \Delta\tau_{ij}$); $D_*^{P,SH}$ is the correction factor, of about two on the average. For SV waves, $\dot{u}(r,t)$ for some directions is a linear combination of $\dot{F}_0(t)$ and the Hilbert transform of $\dot{F}_0(t)$. The shape of the amplitude spectrum will, however, be similar for SV and SH -waves.

The breaking time T_a was determined in DK83 by numerical simulation using a grid model of a circular asperity with diameter $2R_a$ equal to 11 grid units.

Let

$$T_a = \frac{2R_a}{v_a c_S} \quad (3)$$

the simulation in DK83 gave $v_a = 0.65-0.75$. It is not clear, however, whether this estimate can be applied if the asperity is fractured not spontaneously but during the process of rupture propagation along the fault surface. DAY (1982) carried out the numerical simulation for an inhomogeneous dynamical source model which included three isolated loaded patches. For the first patch which was fractured spontaneously the rupture propagation velocity was below c_S ; the second patch was fractured faster, and the third one with rupture velocity considerably above c_S . Therefore we shall assume for further estimates $v_a = 1.35$ (equivalent rupture velocity = $0.79c_P = 1.35c_S$).

The most restrictive idealization of DK83 is the assumption of an infinite fault. In this case the Rayleigh waves generated by the fracture propagate to infinity, and only the above-mentioned displacement step is radiated as body waves. In DK86 the more realistic case of a circular fault is considered, with a circular asperity in its center. In this case, the Rayleigh waves are diffracted at the fault boundaries and are converted into body waves. This leads to changes of wave forms (see case B of Figure 1): a displacement step is concluded by slow return to zero, forming a pulse with characteristic duration of about $2R_s/c_R$, where R_s is the crack radius and c_R is the Rayleigh wave velocity. As one can derive from BOATWRIGHT (1987), these results of DK86 remain generally applicable to an asymmetrically situated asperity on a circular fault (case C, see Figure 1 for minor changes of pulse and spectral shapes).

From now on we shall try to obtain formulas to be used in interpretation of real data. To estimate the numerical factors, we shall use in each case the simplest arbitrary example function. These functions were chosen carefully, so that the related inner incompatibility could be considered negligible when compared to other simplifications of the model.

The first important property of the asperity model is the fact, that the far-field peak acceleration produced by it is determined mainly by stress drop, and does not depend on its size. (It depends however on the shape functions of the space-time history of breaking.) To obtain rough estimates, let us assume that this history and observation direction are such that the radiated velocity pulse shape is a cosine bell

$$f(t) = \begin{cases} 1 - \cos(2\pi t/T), & t \in (0, T) \\ 0 & , \quad t \notin (0, T) \end{cases}.$$

Also, let the asperity shape be circular, with seismic force $F_0 = \pi R_a^2 \Delta\tau$. For the assumed pulse, as one can easily show, $\ddot{F}_{0\max} = \ddot{F}_0(t)_{\max} = 2\pi F_0/T$. Assuming $T = T_a$ and substituting $\ddot{F}_{0\max}$ into the version of (2) for $\ddot{u} = a$, we obtain for peak acceleration in *SH* waves

$$a_{\max}^{SH} = \left(\frac{\pi D^{SH} v_a^2}{8} \right) \frac{\Delta\tau}{\rho r}. \quad (4)$$

Now let us modify this estimate in order to apply it to the interpretation of actual observations of peak acceleration. To attain this, we replace at first D^{SH} by root mean square average,

$$D = \left(\frac{1}{8\pi} \int_{\Omega} ((D^{SH})^2 + |D^{SV}|^2) d\Omega \right)^{1/2} \quad (5)$$

where Ω is the unit sphere. Our rough estimate of D gave $D = 1.16$ ($D_* = 2.6$). The free surface correction factor of two should be also added, and at last we should account for impedance ($c_s\rho$) difference between the source and receiver (see GUSEV, 1983). For typical frequencies of 3–10 Hz this correction also nearly doubles the amplitude. The final formula at $v_a = 1.35$ is

$$a_{\max} = 3.3\Delta\tau/\rho r. \quad (6)$$

HANKS and JOHNSON (1976) obtained an analogous estimate (with a factor of 1) from general dimensional considerations.

Let us consider now the spectra of radiated waves (see Figure 1). Characteristic frequencies f_a and f_c are determined by the displacement step/pulse rise time T_a and by the displacement pulse duration T_s :

$$f_{a,c} = C_B/T_{a,s} \quad (7)$$

where we shall assume further $C_B = 0.8$ which is accurate for a symmetrical trapezoidal pulse with rise/decay time equal to 20% of its total duration. For the case *A* at frequencies $f \ll f_a$, the amplitude spectra of velocity and acceleration are

$$\begin{aligned}\dot{u}(f) &= u(t)|_{t=\infty} = DF_0/4\pi\rho c_S^2 r \\ a(f) &= \ddot{u}(f) = 2\pi f \dot{u}(f).\end{aligned}\quad (8)$$

These formulas remain approximately true also for the case *B*, in the interval $3f_c < f < f_a/3$. Therefore the level of velocity spectrum (and the value of acceleration spectrum at a given frequency) are determined in this frequency range by the seismic force F_c only. For the neighbourhood of frequency f_a , let us represent approximate acceleration spectrum (by analogy with the known Brune's spectral shape) as

$$a(f) = \left(\frac{DF_0}{2\rho c_S^2 r} \right) \frac{f}{1 + (f/f_a)^{\gamma_a}}. \quad (9)$$

Here we must fix the value γ_a of high-frequency slope. For cosine bell velocity pulse $\gamma_a = 3$, but this guess is misleading because we chose this shape arbitrary to exclude acceleration jumps; this automatically leads to $\gamma_a = 3$. We found no definite theoretical considerations to fix γ_a at present; all values between 1.5 and 3.5 seem more or less probable, and the choice of any value in this range does not change radically the results below. Based on some experimental spectra (see *e.g.*, FACCIOLI, 1986), we fix $\gamma_a = 2$, and for the peak value of acceleration spectrum we obtain

$$a(f)_{\max} = \frac{DF_0 f_a}{4\rho c_S^2 r}. \quad (10)$$

Hence, $a(f)_{\max}$ is related to $F_0 f_a$, or to $\Delta\tau R_a$; the last conclusion corresponds to equation (6b) of BOATWRIGHT (1987). Note that on Figures 1 and 3 corners are drawn instead of smooth peak discussed here.

From the point of view of fault mechanics, an important problem is that of stress concentration at the asperity. In the model of DK83 the initial conditions are of zero displacement jump over the asperity, and loading is caused by displacement at infinity. This assumption leads to an (integrable) singularity of stress at the boundary of the asperity (and maybe also to the specific "double pincer" fracture mode). One can suggest however that real asperities can "plastically accommodate" to the load, so that the stress distribution over the asperity area is considerably smoother. The same conclusion can be obtained from the analysis of another model of an asperity, namely an elastic paraboloidal hill pressed on an elastic half-space. This problem is identical to the well-known Hertz's problem of the contact of elastic spheres (GALIN, 1980). For a cohesionless contact, the theory predicts an ellipsoidal profile of normal stress (similar to the profile of displacement jump for

a circular crack). One can assume that if dry friction and shear load are added, the arising shear stress will have a qualitatively similar profile (stress increasing from the boundary to the center and not otherwise). Detailed analysis of this case is somewhat difficult: one should explicitly take into account the history of loading. Note also that in this context, the asperity model of DK83 can be compared with a "flat-top hill with shear slopes".

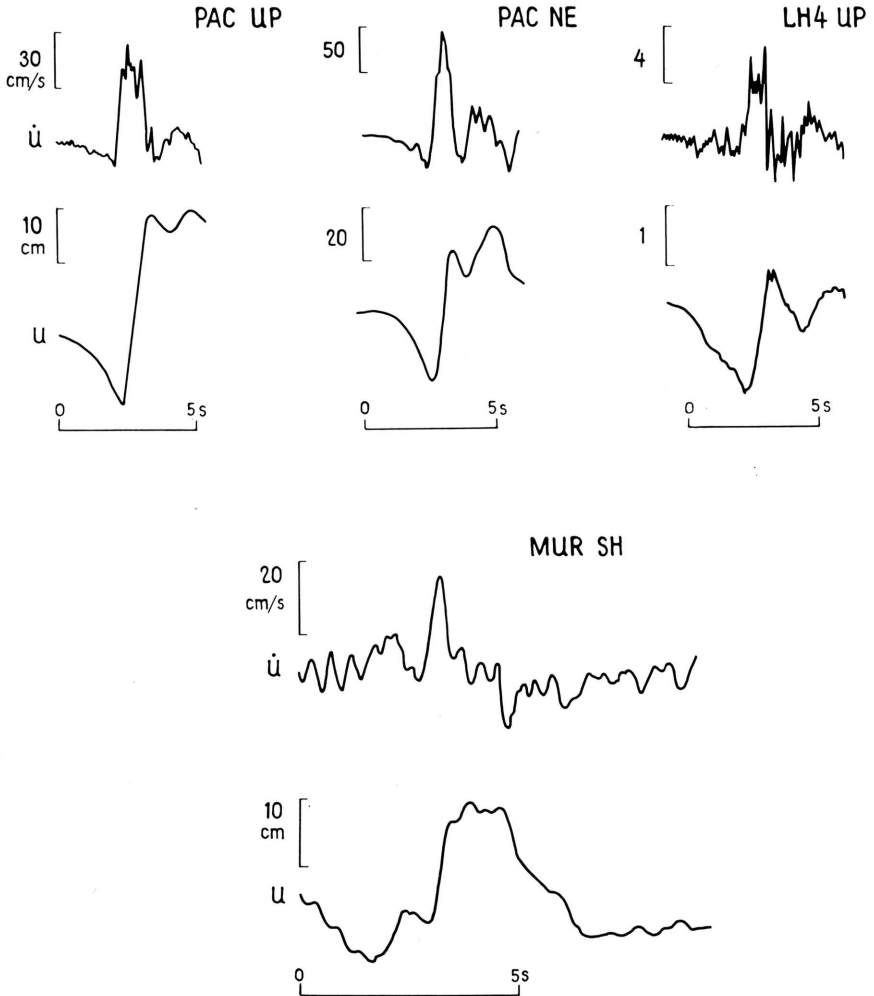


Figure 2

Wave forms of waves radiated supposedly by breaking of asperity. Above—for asperity in the deeper part of the source of the San-Fernando earthquake of 1971. Single and double integrated accelerograms are plotted for stations Pakoima and Lake-Hughes-4 (HEATON and HELMBERGER, 1979). Below—same plots for the Tokachi earthquake of 1968, for station Muroran (pulse No. 2) (MORI and SHIMAZAKI, 1984). In all cases one can see unipolar velocity pulse and displacement step (more or less deformed during stabilized double integration).

Table 1
Parameters of asperities calculated from wave forms of Fig. 2¹

Event	Station, component	r km	u cm	T_a s	$\log F_0$ dyne	R_a km	$\Delta\tau$ bar
San-Fernando, 1971	Pacoima, up Lake Hughes 4, up	14 25	35 ² 2	1.5 1.0	19.93 18.94	2.6 1.7	400 90
Tokachi-oki, 1968	Muroran, <i>SH</i>	160	9	0.9	20.41	2.1	1800 ³

¹ Calculation was carried out using (2) and (3), taking into account free surface factor of 2; $c_s = 3.5$ km/s, $\rho = 2.7$ g/cm³, $D = 1.16$, $\nu = 1.0$ for the San-Fernando and $\nu_a = 1.35$ for the Tokachi event.

² u , and consequently F_0 and $\Delta\tau$ are possibly exaggerated because of local topography. Note that both estimates for the San-Fernando event correspond to the same asperity.

³ Anomalously powerful pulse.

Now we present two examples of records where radiation may be assumed to be due to single breaking asperities. A distinctive feature of such a record is a unipolar velocity pulse. Both examples were found in integrated accelerograms of large earthquakes. A velocity pulse can be clearly identified in such a record in two cases: either it should be one of only a few pulses, or it should be anomalously strong. Both cases are observed in examples. The first example (see Figure 2) was mentioned by HANKS and JOHNSON (1976) (reproduced from HEATON and HELMBERGER, 1979). Another probable pulse due to an asperity was found by MORI and SHIMAZAKI (1984) who ascribed it to a crack subsource. Our interpretation seems equally well founded. The estimates of parameters F_0 , R_a and $\Delta\tau$ for both examples are given in Table 1.

3. Elastic Waves From a Multiasperity Source

As one can see from the preceding section the main velocity or acceleration pulse from a single breaking asperity is determined by its "local" properties (mainly by stress drop and size). Hence we can assume that in case of several adjacent breaking asperities as a first approximation we can calculate SP radiation separately for each asperity and then add the results.

Let us consider a fault model consisting of a crack with many small contact patches (asperities). Macroscopically such a model is equivalent to the usual fault model with cohesion. It can be specified by, e.g., cohesive stress (or static friction or strength), σ_{coh} and residual friction σ_{fr} . These macroscopic parameters are in fact determined by the properties and configuration of the mentioned contact patches. The same is true with respect to macroscopic fracture criterion. As for short-period radiation accompanying fracture, it cannot be correctly described at this "macro"-level: this is a fully "microscopic" phenomenon.

Consider now an earthquake source situated on such a fault. Let it “macroscopically” be a shear crack (*e.g.*, the circular crack of radius R_s with constant stress drop $\Delta\sigma$). During the formation of the crack its tip (*i.e.*, rupture front) propagates “macroscopically smoothly”, but “microscopically” this rupture propagation is a wave of breaking of asperities. We shall name such source model the multiasperity model.

Macroscopic stress drop $\Delta\sigma$ can be determined in this model only for a considerably large region of a fault surface containing many asperities. Constancy of $\Delta\sigma$ over the source area means that the mean $\Delta\sigma$ is the same for any such region. The relation between macroscopic $\Delta\sigma$ and average stress drop $\Delta\tau$ over an asperity for a given source is determined from a condition of correspondence of forces between microscopic and macroscopic representations. For similar asperities this gives

$$S\Delta\sigma = \sum_i F_{0i} = N\Delta\tau S_a \quad (11)$$

where S is the source area, N is the number of asperities over it, and $\Delta\tau$ and S_a can be considered as average values over the set of asperities.

Using the filling factor k_f introduced above we can represent N as

$$N = k_f S / S_a = k_f R_s^2 / R_a^2 \quad (12)$$

The last equality is valid for a circular source of radius R_s and for circular asperities of identical shape; we shall base our estimates on this case. From (11) and (12) we can now relate $\Delta\sigma$ and $\Delta\tau$ simply as

$$\Delta\tau = \Delta\sigma / k_f \quad (13)$$

This intuitively obvious relation agrees well with the strict results of BOATWRIGHT (1987) who derived the formula for the average seismic moment created by some definite asperity (be it a single one or one among others) situated at a random place over a circular crack which in our notation is

$$M_{01} = \frac{16}{7} R_a^2 R_s \Delta\tau = \frac{16}{7\pi} R_s F_0 \quad (14)$$

where R_s is the crack radius and M_{01} is the seismic moment produced by a single asperity failure. Expressing the total seismic moment M_0 of the source as $M_0 = NM_{01}$ and as $M_0 = (16/7)R_s^3 \Delta\sigma$ one can easily derive (13). We shall need also below the average distance between asperities which we shall determine as

$$d = (S/N)^{1/2} = (\pi/k_f)^{1/2} R_a \quad (15)$$

Let us assume that breaking of each asperity begins at a random moment of time. Then for a source in which N asperities are broken, the SP acceleration amplitude spectrum will be

$$a(f) = a_1(f)N^{1/2} \quad (16)$$

where $a_1(f)$ is the average spectrum for a single asperity.

Note that after the rupture front has gone and has “freed” a given point of a fault, slip of fault walls can progress either smoothly or as stick-slip (with temporal interlocking). In the second case, several SP pulses can be generated by the same asperity before healing. If this phenomenon is real, the estimate (16) is incorrect, and $a(f)$ is proportional not to S but to ST_s , where T_s is the duration of the earthquake source process. Assuming similitude as is often done (see *e.g.*, GUSEV, 1983) these two cases lead to either $a(f) \propto M_0^{1/3}$ (when (16) is valid) or $a(f) \propto M_0^{1/2}$ (in the second case). In (GUSEV, 1983) the second case was assumed, and the postulate of constant “effective” $\Delta\sigma$ of HANKS and MCGUIRE (1981) implicitly assumes the first case. Note that empirical SP spectral trends compiled by GUSEV (1983) corresponded to $a(f) \propto M_0^{0.36}$; but more recent data of KOYAMA and ZHENG (1985) and HOUSTON and KANAMORI (1986) lead to $a(f) \propto M_0^{0.42-0.47}$. Therefore observational data are not fully decisive here. Important in this respect are the results of SPUDICH and CRANSWICK (1984) who by means of a phased array managed to track the movement of the “bright” SP radiator at the propagating rupture front. Taking this into account we are inclined here to the first variant (asperity radiates once) and we relate the difference of the observed exponent from 1/3 to some secondary factors. This point cannot, however, be considered as fully settled.

Let us consider now the general structure of the source radiation spectrum in the multiasperity model. As in GUSEV (1983) we shall assume that the “macroscopic” crack radiates a smooth unipolar displacement pulse. The spectrum of this pulse has a corner frequency f_c and high-frequency asymptote of the type $f^{-\gamma}$ with $\gamma = 2.5-3.5$. The SP radiation from breaking asperities is superposed onto this smooth pulse. Note that in the present model, the total SP radiation energy increases, with increasing source size, in proportion to its area S (and not to ST_s as in GUSEV, 1983). Thus, SP radiation energy, if treated at the “macroscopic” level, can be included into fracture energy, or in “quasi-thermal” losses (KOSTROV, 1975).

To present a wide-band radiation spectrum most clearly, following GUSEV (1983), we introduce the modified source spectrum

$$K(f) = f^2 \dot{M}_0(f) \quad (17)$$

where the more common source spectrum $\dot{M}_0(f)$ is the Fourier transform of $\dot{M}_0(t)$, *i.e.*, the seismic moment rate of the equivalent point double dipole. The shape of

$K(f)$ immediately defines an acceleration spectrum of S -waves

$$a(f) = \frac{(2\pi)^2 \mathcal{R}K(f)}{4\pi\rho c^3 r}. \quad (18)$$

This is a slightly modified standard result for a homogeneous infinite medium. \mathcal{R} is generally the full-vector S -wave radiation pattern for a given ray, but to obtain average results for all directions we can consider \mathcal{R} as spherical rms value. Same is true for D and D_* values below. As usually we neglect P -wave contribution to accelerations.

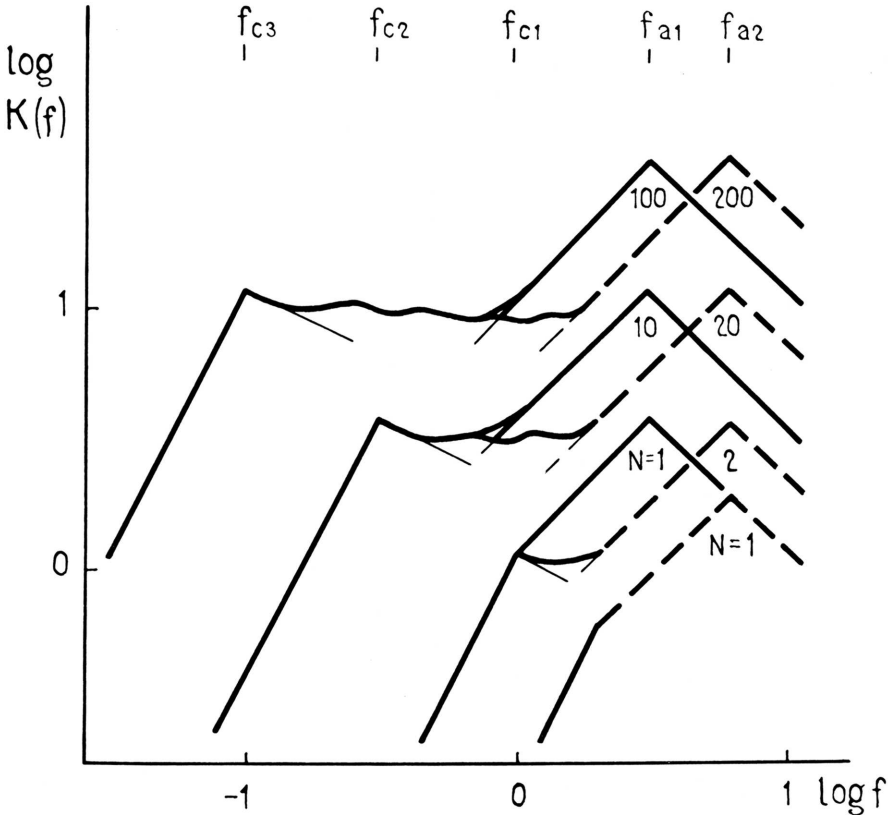


Figure 3

Schematic scaling laws of source spectra $K(f) = f^2 M_0(f)$ for multiasperity source model. Similitude is assumed for the main “macroscopic” source/crack and for its rupture history: $\Delta\sigma = \text{const}$, $f_c \propto M_0^{-1/3}$. The relative f_c values presented are: $f_{c1} = 1$, $f_{c2} = 0.316$ and $f_{c3} = 0.1$; they correspond to $M_0 = 1, 31.6$ and 1000 . The asperity number $N \propto S \propto M_0^{2/3}$. Some definite values of $\Delta\tau$ and k_f are assumed, and two different values of f_a are fixed giving two scaling laws. The spectra of single-asperity sources are marked by $N = 1$, they are fully similar. At given f_a , $K(f)_{\text{max}} = K(f_a)$ grows as $N^{1/2}$ because of incoherency, leading to $K(f)_{\text{max}} \propto M_0^{1/3}$. At given M_0 and f_c , $K(f)_{\text{max}}$ is independent of f_a . Low-frequency (coherent “macroscopic”) spectral shape assumedly has $f^{-0.5}$ asymptote. Coherent and incoherent parts of the spectrum are schematically connected by a wavy line.

Several schematic $K(f)$ spectra are plotted in Figure 3, including that of a small earthquake which within the frames of our fault model should be compared with the breaking of a single asperity. As is clearly seen from Figure 3, the proposed model leads to spectral scaling law with no similitude, and the kind of violation of it agrees with the revised B model of AKI (1972) and with spectral shapes suggested in GUSEV (1983).

Combining (16) and (18) with (8) or (9) one can easily estimate $K(f)$ for the multiasperity model with similar asperities. For the intermediate frequency f^1 slope of $K(f)$ below f_a we obtain

$$K(f) = 0.5D_*c_s k_f^{1/2} R_s R_a \Delta\tau f. \quad (19)$$

For the neighbourhood of f_a , i.e., near the peak of $K(f)$, assuming $\gamma_a = 2$ and having determined from (4) and (7)

$$R_a = v_a c_s C_B / 2f_a \quad (20)$$

we obtain

$$K(f)_{\max} = K(f_a) = 0.125D_*c_s^2 k_f^{1/2} C_B v_a R_s \Delta\tau. \quad (21)$$

Note that (19) implies the general relation $K(f) \propto R_a \Delta\tau$ but (21) implies another relation for the spectral peak, namely $K(f)_{\max} \propto \Delta\tau$.

4. Statistical Properties of Asperity Stress Drop and the Structure of Accelerograms

In this section we shall derive an estimate of the asperity stress drop $\Delta\tau$ based on peak acceleration data. We shall assume that the peak value of acceleration is produced by a pulse from some definite asperity and not as a fluctuation of a certain random sum. This assumption will be justified below. In these and all the further calculations we shall use the same set of parameters: $D = 1.16$, $D_* = 2.6$, $C_B = 0.8$, $v_a = 1.35$, $k_f = 0.1$, $\rho = 2.7 \text{ g/cm}^3$, $c_s = 3.5 \text{ km/s}$, and assume the typical $\Delta\sigma$ value to be 30 bars. The choice of k_f value is mostly arbitrary except that the above-mentioned conditions $k_f < 0.3$ was taken into account. The value $k_f = 0.1$ seemed to be a reasonable starting value. The realistic range of k_f will be estimated in the concluding part of the paper. Also we shall assume the f_a value to be 2.4 Hz based on observations described below, through (20) it entails $R_a = 0.8 \text{ km}$. The values of k_f and $\Delta\sigma$ provide us, through (13), with the first empirical estimate of $\Delta\tau$: $\Delta\tau_1 = 300 \text{ bar}$.

The multitude of asperities of a fault or faults can be considered as a statistical ensemble with distribution function

$$P(\Delta\tau' > \Delta\tau, R_a^1 > R_a) = F(\Delta\tau, R_a).$$

Only $\Delta\tau$ distribution will be discussed below. Remember that $\Delta\tau$ determines the peak acceleration of a pulse generated by the breaking of a single asperity. "Heavy tails" of strength distributions for relatively successful models of real faults (e.g., MIKUMO and MIYATAKE, 1978) and the specific appearance of accelerograms recorded in the vicinity of faults suggest a powerlaw (not Gaussian or lognormal) distribution for $\Delta\tau$:

$$P(\Delta\tau' > \Delta\tau) = (\Delta\tau/\Delta\tau_{\min})^{-\alpha}. \quad (22)$$

We shall need the expression for the median $\Delta\tau_{N_0,0.5}$ of a maximum value in a sample of size N_0 for this distribution. Calculation gives

$$\Delta\tau_{N_0,0.5}/\Delta\tau_{\min} = (1 - 2^{-1/N_0})^{-1/\alpha} \approx (1.45N_0)^{1/\alpha}. \quad (23)$$

Mean value and variance for (22) are

$$\langle\Delta\tau\rangle = \left(\frac{\alpha}{\alpha-1}\right)\Delta\tau_{\min} \quad (24)$$

$$\langle(\Delta\tau - \langle\Delta\tau\rangle)^2\rangle = \left(\frac{\alpha}{(\alpha-1)^2(\alpha-2)}\right)(\Delta\tau_{\min})^2. \quad (25)$$

We shall apply these results to the interpretation of peak acceleration data obtained near a fault/source. To start with, we shall assume that at a receiver point at the Earth's surface, at distance r_0 from the surface of a supposedly vertical fault, one can determine the peak acceleration a_{\max} taking into account only the contribution of the nearest part of the fault surface because the radiation from farther points of the source will not produce a maximum pulse. This means that the size or the magnitude dependence of a_{\max} (at given r_0) exists for small shocks only, such that their source surface cannot cover this nearest part of the fault and saturates for the size and M values above some critical value (cf., CAMPBELL, 1981). This value (M_{cr}) can be determined from the area of the mentioned fault region. To obtain numerical estimates, we shall consider this region to be the lower half of a vertical square with side $2r_0$, and with its center on the Earth's surface at the point of the fault which is the nearest to the receiver. The area of this region is $2r_0^2$. The mean distance from a random point of this region to the receiver is $\bar{r} \approx 1.2 r_0$.

Let us fix r_0 to be 10 km; then the assumed area of the nearest region of the fault surface is $S = 200 \text{ km}^2$ which corresponds to $M_{\text{cr}} \approx 6.3$. For lower magnitudes, median peak acceleration (which is proportional to $\Delta\tau_{\max}$, see (6)) will decrease with decreasing M because the number $N_0 = N$ of asperities in (23) is

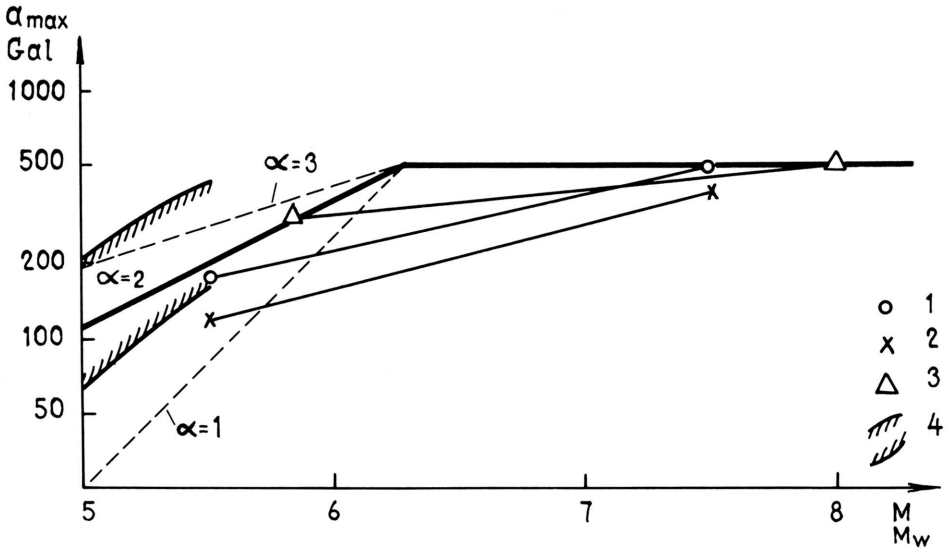


Figure 4

Empirical relations between peak horizontal acceleration a_{\max} on the rock and magnitude, and theoretical broken lines for distance $r_0 = 10$ km from a fault or source surface, for power law $\Delta\tau$ distributions with exponent $\alpha = 1.2$ (recommended) and 3. Empirical plots are drawn in their intervals of applicability: 1—after DONOVAN and BORNSTEIN (1978), 2—after CAMPBELL (1981), both 1 and 2—for a distance of 10 km from the nearest point of the vertical projection of a fault onto the Earth's surface; 3—after (GOTO *et al.*, 1984) for epicentral areas; 4—data range of (FACCIOLI, 1986) for a hypocentral distance of 10 km.

getting lower. As $N \propto S$, $\log a_{\max} \propto \frac{1}{\alpha} \log S$, and also $\log S \approx M + \text{const.}$, so that we can relate a_{\max} to M at $M < M_{\text{cr}}$. On Figure 4 empirical relations (a_{\max}, M) are plotted for $r_0 = 10$ km, each in its interval of validity, and their approximation by the “theoretical” broken lines

$$\log a_{\max}(M) = \begin{cases} \frac{1}{\alpha} (M - M_{\text{cr}}) + \log \hat{a}, & M \geq M_{\text{cr}} \\ \log \hat{a}, & M < M_{\text{cr}} \end{cases} \quad (26)$$

drawn for $\alpha = 1, 2$ and 3. Obviously $\alpha = 2$ is a rough estimate; but values $\alpha = 1$ and $\alpha = 3$ are clearly less preferable. The reasonable agreement between empirical data and theoretical prediction supports our theory. The estimated \hat{a} level can be used to find out an estimate of $\Delta\tau$ employing (6) and assuming the mentioned correspondence between peak acceleration and the strongest asperity. Inverting (6) for a random location of this asperity we obtain the stress drop estimate

$$\Delta\tau_{\max} = 0.30\rho\bar{r}a_{\max}. \quad (27)$$

To obtain average $\Delta\tau$ we assume that $\Delta\tau_{\max}$ corresponds to $\Delta\tau_{N,0.5}$ then (23) and (24) give

$$\langle\Delta\tau\rangle = \frac{\alpha}{\alpha - 1} \left(\frac{\pi R_a^2}{1.45 k_f (2r_0^2)} \right)^{1/\alpha} \Delta\tau_{\max}. \quad (28)$$

Assuming here $\langle\Delta\tau\rangle$, R_a and k_f to be constant, one can derive from (27) and (28)

$$a_{\max} = f(\alpha) r_0^{(2/\alpha) - 1}. \quad (29)$$

This means that when $\alpha = 2$, the average peak acceleration near the middle part of an elongated source does not depend on the fault distance (up to distances which are near to the fault width). This conclusion seems to be supported by macroseismic data providing an independent confirmation of our estimate $\alpha = 2$. Now assuming $\alpha = 2$, $\bar{r} = 1.2r_0 = 12$ km and $\hat{a} = 500$ cm/s², we obtain the second experimental estimate of $\Delta\tau$: $\Delta\tau_2 = \langle\Delta\tau\rangle = 260$ bar.

Now we proceed to the problem of acceleration peaks, which is important in particular because there is a widely used representation of an accelerogram as a quasistationary Gaussian process. We shall begin with a general case. Consider a rectangular $L \times W$ source with a rupture propagating along its longer side L at the velocity $v = v_s c_s$ so that the total rupture time is $T_s = L/v$. Then the number of asperities broken during a time interval of duration T_a is

$$m = \frac{NT_a}{T_s} = \frac{2K_f v_s W}{\pi v_a R_a} = \frac{4k_f v_s W f_a}{\pi v_a^2 C_B c_s}. \quad (30)$$

When $m \lesssim 1$, pulses do not overlap, at least near the source, and the accelerogram appearance will be specific. As the epicentral distance increases, scattering and multipathing will normalize an accelerogram making it look more like a Gaussian process. The value $m = 1$ corresponds to the critical source width

$$W_{\text{cr}} = \frac{\pi v_a^2 C_B c_s}{4k_f v_s f_a}. \quad (31)$$

At reasonable $v_s = 0.6$, $W_{\text{cr}} \approx 30$ km. Hence, multiple overlapping of pulses can take place for great earthquakes only.

Even in this case, however, the accelerogram will not be near to the Gaussian process, if $\alpha \approx 2$. As one can see from (25), when $\alpha \leq 2$, the distribution (22) has no finite variance. Hence, even in the case of multiple overlapping pulses the main contribution to the peak amplitude will come from a certain single asperity. This conclusion justifies our previous assumptions. One can say somewhat exaggeratedly that each positive or negative swing on an accelerogram corresponds to some individual asperity. The results presented in this section can obviously be used for accelerogram synthesis.

5. Statistical Properties of Asperity Stress Drop and Barriers on a Fault

There is another, theoretical way to derive the $\Delta\tau$ distribution if one employs the ideas of FUKAO and FURUMOTO (1985). They believe (we shall drop some important but irrelevant details) that an earthquake source grows in approximately self-similar steps or stages, so that its current size takes the sequential values of a geometric series L_0, hL_0, h^2L_0, \dots . At each stage the barrier situated along the instant source perimeter is broken. This occurs in a mode which is close to critical, with a large probability of stopping. Linear barriers of different strengths form on a fault surface a hierarchical system of grids with different cell sizes so that the larger the cell size the stronger are the constituent linear barriers. At each definite stage of its growth the source occupies one (or several) cell of the corresponding hierarchical range.

We shall assume that barriers of this model are in fact chains of strong asperities situated at distance d from each other. Consider some definite region of fault surface of area S^* . The total length of grid sides for a grid with a square cell of size q can be determined as (number of cells) \times (cell half-perimeter) giving $(S^*/q^2) \cdot 2q = 2S^*/q$. Then the number of asperities in this grid is $N^*(q) = 2S^*/qd$. Specifying our initial assumption, let the average $\Delta\tau$ of these asperities ($\Delta\tau_B$) be proportional to q^β , then

$$N^*(\Delta\tau_b) \propto \Delta\tau^{-1/\beta}. \quad (32)$$

In order to relate q to $\Delta\tau_b$ let us consider the known equilibrium relation for a crack with a finite edge zone (Barenblatt-Dugdale model):

$$\Delta\sigma_e \approx (R_s/a)^{1/2} \Delta\sigma \quad (33)$$

where $\Delta\sigma$ is the stress drop over the area of a circular crack of the radius R_s , and $\Delta\sigma_e$ is (cohesion minus friction) over the ring-like edge zone (cohesion zone) of width $a \ll R_s$. To derive a "microscopic version" of this criterion, let us take into account the chain interval of d , and let the distance between "rows of asperities", also equal to d , correspond to the cohesion zone width a . The condition of correspondence of forces then gives $\Delta\sigma_e d^2 = \Delta\tau_b S_a = \Delta\tau_b k_f d^2$ so that the criterion for breaking of a link of asperity chain becomes

$$\Delta\tau_b = (R_s/d)^{1/2} (\Delta\sigma/k_f). \quad (34)$$

We shall assume that the barrier fails when this criterion is satisfied for average $\Delta\tau_b$ of the chain elements. Then assuming that (34) relates the cell size of barrier grid $q \approx 2R_s$ to the $\Delta\tau_b$ value of barriers in this grid we find out that β in (32) is equal to $1/2$. Hence for probabilities of different $\Delta\tau_b$ values we obtain

$$P(\Delta\tau_b) \propto \Delta\tau_b^{-2}.$$

Remember now that $\Delta\tau_b$ values and q values form a geometrical series. Then

$$P(\Delta\tau'_b \geq \Delta\tau_b) \propto \frac{1}{\Delta\tau_b^2} + \frac{1}{h\Delta\tau_b^2} + \frac{1}{h^2\Delta\tau_b^2} + \dots = \frac{1}{\Delta\tau_b^2} \left(\frac{1}{1-1/h} \right) \propto \Delta\tau_b^{-2}. \quad (35)$$

We cannot of course expect that all strong asperities with some definite $\Delta\tau$ belong to barriers-chains. It is sufficient to suppose that the fraction of asperities with given $\Delta\tau$ which belong to barriers is independent of $\Delta\tau$. Then (35) can be directly compared with (22), and we obtain the additional support to our assumption of a power-law on distribution of $\Delta\tau$ with $\alpha = 2$ (see eq. (22)).

We assumed implicitly that $\Delta\sigma$ is constant for each stage of the source growth. This is the consequence of our fault model and also agrees with observed general independence of $\Delta\sigma$ on L for real earthquake sources of different sizes which according to ideas of FUKAO and FURUMOTO (1985) can be considered as certain "frozen" stages of growth of larger sources.

Now we shall construct an estimate of average $\Delta\tau$ based on presented considerations. Let us assume that the distribution (35) is also valid for a set of N_p asperities constituting the part of the perimetric barrier which is near to failure (or is broken in an almost critical mode). Assume this part to be half of the perimeter. For a circular source, $N_p = \pi R_s/d$. For the average of N_p values of $\Delta\tau_b$ (denote it $\Delta\tau_p$), (34) is valid. For the strongest of N_p asperities taking into account (23) and (24), the median $\Delta\tau$ is

$$\Delta\tau_M = \frac{1}{2} \Delta\tau_p (1.45 N_p)^{1/2}. \quad (36)$$

The similar formula

$$\Delta\tau_M = \frac{1}{2} \langle \Delta\tau \rangle (1.45 N)^{1/2} \quad (37)$$

relates $\Delta\tau_M$ to $\langle \Delta\tau \rangle$ (*i.e.*, the average $\Delta\tau$ for the whole source), if we make a rather likely assumption that the strongest of N asperities is situated on the perimeter. Combining these results, we obtain

$$\langle \Delta\tau \rangle = \Delta\tau_p (N_p/N)^{1/2} = \Delta\sigma/k_f. \quad (38)$$

This coincides with (13). Thus we have not obtained any new estimate of $\Delta\tau$; we have demonstrated however the lack of inner contradictions of our model in this respect.

The use of static crack-tip models in this section and its correspondence with a multiasperity model can rise a question on the general relation between the presented multiasperity model and the crack-tip movement models of SP seismic

energy radiation, such as that of MADARIAGA (1983). These models are logically different. In the crack-tip movement model, the SP power is produced by variations of crack-tip velocity, which is here a well-defined parameter. In our model, the crack-tip is seen only macroscopically and it disintegrates at close view. Its movement is a movement of a signal for asperities to break. Each asperity breaks autonomously, and SP energy is therefore largely independent of (macroscopic) crack-tip velocity at all, moreover of its local variations which are ill-defined in this model.

6. Empirical Source Spectra and the Multiasperity Model

We shall compare now the empirical $K(f)$ functions with those expected from our model (Figure 3). In order to find empirical $K(f)$ we used average horizontal acceleration spectra for large earthquakes of "Western USA" region (WUSA) and of Japan, and also three anomalous acceleration spectra: for the great Peruvian earthquakes of 1966 and 1970 recorded in Lima (CLOUD and PEREZ, 1971) with unusually high amplitudes, and of low-amplitude record of the Ust-Kamchatsk earthquake of 1971 (SHTEINBERG *et al.*, 1975).

Functions $K(f)$ were calculated in the following way. For individual records, the Fourier amplitude spectra of the two horizontal channels were averaged and smoothed, then they were reduced to $r = 50$ km using the attenuation function $r^{-1} \exp(-\pi fr/c_S Q(f))$, with

$$Q(f) = \begin{cases} Q_0(f/f_0)^{0.8}, & f > f_0 \\ Q_0, & f < f_0 \end{cases} \quad (39)$$

where $Q_0 = 314$, $f_0 = 1$ Hz and $c_S = 4.3$ km/s.

Average regional spectra of horizontal acceleration for a rock site were also determined for $r = 50$ km. For WUSA, we used data of TRIFUNAC and LEE (1985) for $M_L = 5.7$ and 6.6; for Japan—data of GOTO *et al.* (1984), for $M_{JMA} = 7.5$. In the last case, $a(f)$ was determined from published parameters $a_m(f)$ and $t_p(f)$ using the formula $a(f) = e = 2.72/2 a_m(\pi t_p)^{0.5}$ derived analytically by ourselves.

Converting of $a(f)$ for $r = 50$ km to $K(f)$ was carried out in the uniform way assuming in (18) that empirical $a(f)$ corresponds to one half the total spectral energy of S waves, taking into account also a free surface factor of two and the average radiation pattern of $(0.4)^{0.5}$. Absorption was corrected using (39) with $Q_0 = 160$ and $f_0 = 1.8$ Hz. Medium parameters were those of the average crust as given in Sect. 4 above.

The results are presented in Figure 5. Low-frequency branches of $K(f)$ curves (below f_c) were plotted according to the ω^{-2} spectral model with

$$\log f_c = -1/3(\log M_0 - 23.32). \quad (40)$$

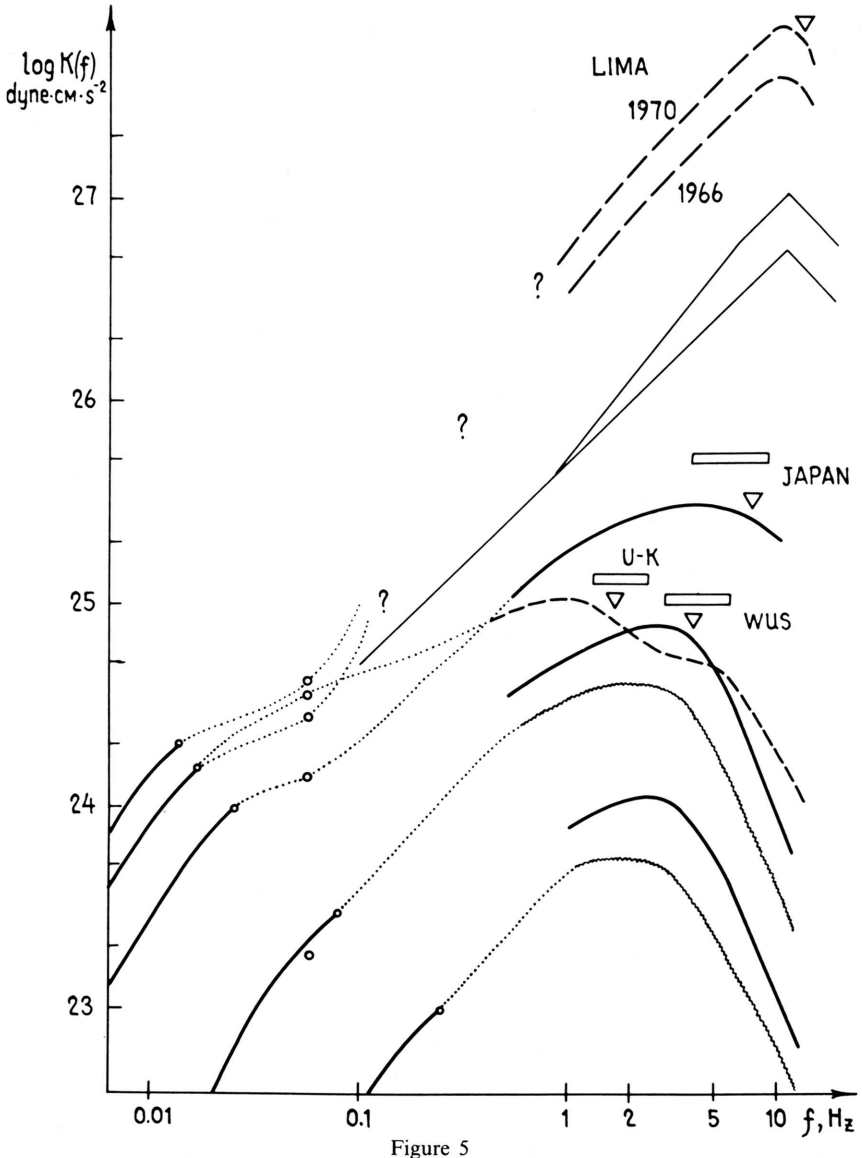


Figure 5

Empirical $K(f)$ spectra. Low-frequency parts are constructed using M_0 and f_c , high-frequency parts—from acceleration spectra, control points at 0.05 Hz—from M_s . Triangles are the estimates of $f_d(f_{\max})$, quadrangles denote the range of typical corner frequencies of small earthquakes in the corresponding regions. From the top to the bottom: spectra of the Peruvian shocks of 1966 and 1970 ($\log M_0 = 28.3$ and 28) recorded in Lima; average spectrum of $\log M_0 = 27.5$ ($M_{\text{JMA}} = 7.5$) shock in Japan; spectrum of the Ust-Kamchatsk earthquake of Dec. 15, 1971, $\log M_0 = 27.9$; average spectra for WUSA, for $\log M_0 = 26$ and 24.5 ($M_L = 6.6$ and 5.7), in two versions: initial (solid line) and reduced to homogeneous crust (zigzag line). The dotted line denotes less reliable parts of spectra determined by interpolation. Thin lines with angular peaks give upper theoretical limit for the Peruvian shocks.

The spectral levels at $f = 0.05$ Hz were estimated from M_s magnitude using the empirical relation

$$\log K(0.05) = M_s + 16.74. \quad (41)$$

The values of M_0 and M_s for individual events are from (PURCARU and BERCKHEMER (1983); for the average spectra, we use $\log M_0 = 24.5$ for $M_L = 5.7$; $\log M_0 = 26$ and $M_s = 6.5$ for $M_L = 6.6$; $\log M_0 = 27.5$ and $M_s = 7.4$ for $M_{JMA} = 7.5$.

When comparing the empirical spectra of Figure 5 with theoretical ones two biasing factors should be kept in mind. Firstly, acceleration spectra (18) in the frequency range of 1–10 Hz underestimate empirical $K(f)$ (about twice) because of the impedance difference between the average crust and the medium immediately beneath a receiver as was noted above. Secondly, the sources of events of $M = 7.5$ or greater in island arcs are situated mainly in the mantle, not in the crust, and the mantle ρ and μ values are normally used in inversion of M_0 . We however used the crustal medium parameters when $a(f)$ was converted to $K(f)$ (for uniformity). The corresponding correction for high-frequency branches of observed $K(f)$ will increase them (about twice) and will practically compensate for the first biasing effect for larger events. Therefore, correction for the first biasing effect was introduced for WUSA spectra only.

One can see from Figure 5 that after this correction the average $K(f)$ spectra for $\log M_0 = 24.5$, 26 and 27.5 all have the slope of about 1 at the left (low-frequency) side of the spectral peak, in agreement with the predictions of the multiasperity model (see Figure 3). Individual spectra demonstrate large dispersion. The spectrum of the Ust-Kamchatsk earthquake at 1 Hz is 0.5 log unit below the average Japanese spectrum for the same M_0 . Its spectral shape is somewhat different from the predictions of the multiasperity model with similar asperities. In this and some other cases a rather wide distribution of asperity sizes can be hypothesized.

The Peruvian spectra, if taken at face value, are above the average Japanese spectrum for the same M_0 by 1–1.2 log units. Thin lines in Figure 5 show the hypothetical upper limit of spectrum for a shock of $M_s = 7.7$ (two variants correspond to B and C cases of Figure 1). One can see that the expected spectral shape for $f_a = 11$ Hz is in good agreement with the observed one but its level is about 0.8 log units higher. We believe that the shape of Lima records reflects the real picture, but their level is exaggerated because of (1) directivity of radiation (both sources are situated north of Lima and ruptured in the southern direction and (2) hypothetical local focusing or amplification of radiation. Macroseismic intensity in 1970 at many points of the Peruvian shore, at source distances of 30–50 km, was no more than 8–9 MM which is a usual value and obviously disagrees with the spectral level of Lima.

We also marked in Figure 5 the upper cutoff frequencies of $K(f)$ spectra (f_2 after GUSEV (1981; 1983) or f_{\max} after HANKS (1982)). As noted in GUSEV (1983),

the characteristic size of fault heterogeneities is regionally specific; this is represented in acceleration spectra as f_2 variation. For the data of Figure 5, the range of f_2 is from 1.8 to 13 Hz. In GUSEV (1983) we noted also that there is a correlation between f_2 and the typical small earthquake size as revealed in its corner-frequency f_{small} . The ranges of the typical f_{small} values of WUSA and Japan (from published data) and for the focal region of the Ust-Kamchatsk earthquake (our data) are marked in Figure 5. One can see that the correlation between f_2 and f_{small} seems rather probable. This correlation makes our idea that small earthquakes are related to breaking of a single asperity more likely.

Generally speaking, $K(f)$ spectra constructed from accelerograms are in reasonable qualitative agreement with the multiasperity model. In this connection we should mention that HOUSTON and KANAMORI (1986) presented source spectra derived from teleseismic P -waves; corresponding high-frequency $K(f)$ levels are markedly lower than the average spectra of Figure 5 and do not agree with the spectral trend f^1 for $K(f)$ (or f^{-1} for $\dot{M}_0(f)$) at frequencies of 0.2–2 Hz. We believe that this difference is produced by some technical problems. One can compare the source spectrum of the San Fernando earthquake of 1971 according to Figure 8 of HOUSTON and KANAMORI (1986) who used teleseismic P data and obtained $K(1 \text{ Hz}) = 1 \cdot 10^{24} \text{ dyne} \cdot \text{cm} \cdot \text{s}^{-2}$, and according to Figure 3 of PAPAGEORGIU and AKI (1985) who used near-field accelerogram data and obtained $K(1 \text{ Hz}) = 5 \cdot 10^{24} \text{ dyne} \cdot \text{cm} \cdot \text{s}^{-2}$. If this difference of 5 times is attributed to underestimation of t^* , one should increase t^* from 0.7 to 1.2 s (at 1 Hz). But we do not know the real causes of this difference. We decided to reject teleseismic spectral estimates considering them less reliable at present.

Now we can use empirical spectral levels to determine $\Delta\tau$ through inversion of formulas (19) and (21). From Figure 5, for $M_0 = 10^{26}$, the corrected $\log K(f = 0.63 \text{ Hz}) = 24.30$; and $\log K(f)_{\text{max}} = 24.52$ at the frequency $f_{\text{peak}} = 2.4 \text{ Hz}$. There must be some size distribution of real asperities leading to some flattening of the theoretical spectral peak. We shall neglect this and suppose that $f_a = f_{\text{peak}}$, and that (21) can be directly used for interpretation; this can lead to some underestimation of $\Delta\tau$. For a circular source with $M_0 = 10^{26}$ and constant $\Delta\sigma = 30 \text{ bar}$, $R_s = 11.4 \text{ km}$; with all other parameters already fixed, this gives $\Delta\tau_3 = 250 \text{ bar}$ from $K(0.63)$ using (19) and $\Delta\tau_4 = 210 \text{ bar}$ from $K(f_a)$ using (21). Of these two values, the second one is somewhat lower as was expected.

7. Discussion

The proposed multiasperity fault model was employed above to obtain several estimates of the average stress drop over asperity area:

$\Delta\tau_1 = 300 \text{ bar}$ —from global $\Delta\sigma$ and assumed k_f value

$\Delta\tau_2 = 260 \text{ bar}$ —from near-field peak acceleration

$\Delta\tau_3 = 250$ bar—from the level of LF-slope of acceleration spectrum

$\Delta\tau_4 = 210$ bar—from the peak value of acceleration spectrum.

Though the reasonable agreement is obvious, one should not forget that important dimensionless parameters k_f and v_a were fixed in an almost *a priori* manner. Note that in all three formulas for $\Delta\tau_{2-4}$ (not given explicitly for $\Delta\tau_3$ and $\Delta\tau_4$) these two parameters appear in the same combination $k_f^{-0.5} v_a^{-1}$, whereas in the formula for $\Delta\tau_1$ we have $k_f^{-1} v_a^0$. Therefore the obtained agreement will not worsen if k_f and v_a values will change in a coordinated manner, so as not to change the combination $k_f v_a^{-2}$ which should be kept equal to 0.055 ($= 0.1/1.35^2$). The reasonable interval for v_a is 0.6–1.5, this gives the interval for k_f to be 0.02–0.125 and for $\Delta\tau$ —1500–250 bar. Both intervals seem marginally acceptable but so high values of average $\Delta\tau$ as 1500 bars and so low values of k_f as 0.02 seem to be not very probable. Therefore we give: $k_f = 0.04$ –0.125, $v_a = 0.85$ –1.5, $\Delta\tau = 750$ –250 bar and $R_a = 0.5$ –0.9 km as our final estimates.

Several other points are worth being underlined. The agreement is observed between the estimates of asperity stress drop distribution based on (a_{\max}, M) relation for low M , on approximate constancy of a_{\max} in the epicentral region and on the source dynamics considerations. Real spectra $K(f)$ include such features as an interval of f^1 growth, peak and upper cutoff frequency f_2 (f_{\max}) which can be expected from the multiasperity model with similar asperities.

If our conclusion on power-law distribution of $\Delta\tau$ (and consequently of accelerogram peaks) will be confirmed, this will mean that the accelerogram description by the quasi-stationary Gaussian process is not fully adequate. Instead one can describe and also simulate an accelerogram by superposition of relatively rare pulses from individual asperities.

We did not discuss in any detail an important problem of size distribution of asperities, but some difference between $\Delta\tau_3$ and $\Delta\tau_4$, the shape of the Ust-Kamchatsk spectrum and the difference between our average R_a estimate and R_a values of Table 1 show that this problem is important; it needs separate research. But the presence of more or less clearly expressed peak in many accelerogram spectra suggests that the present version of the model, with constant R_a , can be thought to be the reasonable first approximation. In general, we believe that the multiasperity model can provide a realistic mechanical model of the fine structure of a fault and also gives us a successful theoretical model of short-period radiation from earthquake sources.

8. Conclusion

1. Breaking of a small (size under 1 km) asperity on an earthquake-generating fault is supposed to be a typical subsource producing a pulse of short-period elastic

waves from a source of a large earthquake and also represents the main component of a source of a small earthquake.

2. Based mainly on the results of DAS and KOSTROV (1983; 1986) a simple theory is proposed for radiation from a single breaking asperity and from the aggregate of asperities broken during rupture propagation. A new notion of "seismic force" F_0 is introduced as the main integral parameter characterizing small breaking asperity.

3. The derived theory provides several ways to determine typical stress drop $\Delta\tau$ over the asperity area. All estimates agree and give the tentative value of $\Delta\tau = 250\text{--}750$ bar.

4. More or less localized peak and an interval of f^1 slope on the low-frequency side of it which are observed in real acceleration spectra are in agreement with the proposed multiasperity model. The position of the peak is determined by the asperity size, and its amplitude mainly by $\Delta\tau$, that is, by the asperity strength.

5. The fracture criterion for Barenblatt-Dugdale crack model is modified for a fault with asperities. This criterion can be combined with the hypothesis of stochastic self-similarity of source growth to derive $\Delta\tau$ distribution of asperities. The distribution is the power-law one with exponent 2, it agrees well with peak acceleration data for the vicinity of a fault.

6. In order to describe and simulate an accelerogram, one can represent it as a sum of weakly overlapping pulses from individual asperities.

Acknowledgement

The author is indebted to Drs. V. M. Pavlov and J. Boatwright and to anonymous reviewers for valuable critical comments. Dr. Boatwright kindly provided (in late 1986) a copy of his preprint (BOATWRIGHT, 1987).

REFERENCES

- AKI, K. (1972), *Scaling law of earthquake source time-function*, Geophys. J. Roy. Astr. Soc. 31, 3–25.
- AKI, K. (1979), *Characterization of barriers on an earthquake fault*, J. Geophys. Res. 84, 6140–6148.
- ANDREWS, D. J. (1980), *A stochastic fault model. 1. Static case*, J. Geophys. Res. 85, 3867–3877.
- BOATWRIGHT, J. (1982), *A dynamic model for far-field acceleration*, Bull. Seismol. Soc. Amer. 72, 1049–1068.
- BOATWRIGHT, J. (1987), *The seismic radiation from composite models of faulting*, Bull. Seismol. Soc. Amer., in press. 78, 489–508
- CAMPBELL, K. W. (1981), *Near-source attenuation of peak horizontal acceleration*, Bull. Seismol. Soc. Amer. 71, 2039–2070.
- CLOUD, W. K. and PEREZ, V. (1971), *Unusual accelerograms recorded at Lima, Peru*, Bull. Seismol. Soc. Amer. 61, 633–640.
- DAS, S. and AKI, K. (1977), *Fault plane with barriers: A versatile earthquake model*, J. Geophys. Res. 82, 5648–5670.

- DAS, S. and KOSTROV, B. V. (1983), *Breaking of a single asperity: Rupture process and seismic radiation*, J. Geophys. Res. 88, 4277–4288.
- DAS, S. and KOSTROV, B. V. (1986), *Fracture of a single asperity on a finite fault: A model for weak earthquakes?* in *Earthquake Source Mechanics* (eds. S. DAS, J. BOATWRIGHT and C. H. SCHOLZ) (Washington, Amer. Geophys. Union) pp. 91–96.
- DAY, S. (1982), *Three-dimensional simulation of spontaneous rupture: The effect of nonuniform prestress*, Bull. Seismol. Soc. Amer. 72, 1881–1902.
- DONOVAN, N. C. and BORNSTEIN, A. E. (1978), *Uncertainties in seismic risk procedures*, J. Geotechn. Div., Amer. Soc. Civ. Eng. 104, GT7, 869–887.
- FACCIOLI, E. (1986), *A study of strong motions from Italy and Yugoslavia in terms of gross source properties*, in *Earthquake Source Mechanics* (eds. S. Das, J. Boatwright and C. H. Scholz) (Washington, Amer. Geophys. Union) pp. 297–310.
- FUKAO, Y. and FURUMOTO, M. (1985), *Hierarchy in earthquake size distribution*, Phys. Earth. Planet. Interiors 37, 35–148.
- GALIN, L. A. (1980), *The contact problems of the theory of elasticity and viscoelasticity*, Nauka, Moscow, 304 pp. (in Russian).
- GOTO, H., SUGITO, M., KAMEDA, H., SAITO, H., and OOTAKI, T. (1984), *Prediction of nonstationary earthquake motions for moderate and great earthquakes on rock surface*, Annuals, Disaster Prevent. Res. Inst., No. 27B–2, 19–48 (in Japanese).
- GUSEV, A. A. (1981), *A descriptive statistical model for earthquake source radiation and its application to short-period strong-motion estimation*, Abstr. 21, Gen. Asmbl. IASPEI, London, Canada, p. A3.20.
- GUSEV, A. A. (1983), *Descriptive statistical model of earthquake source radiation and its application to an estimation of short-period strong motion*, Geophys. J. Roy. Astr. Soc. 74, 787–808.
- GUSEV, A. A. (1986), *On the nature of short-period radiation of an earthquake source*, in *Seismicity and Seismic Prediction in the Far East*, Abstr., Petropavlovsk-Kamchatsky, p. 79 (in Russian).
- HANKS, T. C. (1982), f_{\max} , Bull. Seismol. Soc. Amer. 72, 1867–1879.
- HANKS, T. C. and JOHNSON, D. A. (1976), *Geophysical assessment of peak accelerations*, Bull. Seismol. Soc. Amer. 66, 959–968.
- HANKS, T. C. and MCGUIRE, R. K. (1981), *The character of high-frequency strong ground motion*, Bull. Seismol. Soc. Amer. 71, 2071–2995.
- HASKELL, N. A. (1966), *Total energy and energy spectral density of elastic wave radiation from propagating faults. 2. A statistical source model*, Bull. Seismol. Soc. Amer. 56, 126–140.
- HEATON, T. H. and HELMBERGER, D. V. (1979), *Generalized ray models of the San-Fernando earthquake*, Bull. Seismol. Soc. Amer. 69, 1311–1341.
- HOUSNER, G. W. (1955), *Properties of strong ground motion earthquakes*, Bull. Seismol. Soc. Amer. 45, 197–218.
- HOUSTON, H. and KANAMORI, H. (1986), *Source spectra of great earthquakes: Teleseismic constraints on rupture processes and strong motion*, Bull. Seismol. Soc. Amer. 76, 19–42.
- KOSTROV, B. V. (1975), *The Mechanics of Source of a Tectonic Earthquake* (Nauka, Moscow) pp. 176 (in Russian).
- KOYAMA, J. and ZHENG, S.-H. (1985), *Excitation of short-period body waves by great earthquakes*, Phys. Earth. Planet. Interiors 37, 108–123.
- LAY, T., KANAMORI, H., and RUFF, L. (1982), *The asperity model and the nature of large subduction zone earthquake*, Earthq. Predict. Res. 1, 3–71.
- MADARIAGA, R. (1983), *Earthquake source theory—a review*, in *Earthquakes: Observation, Theory and Interpretation* (ed. E. BOSCHI) (Corso 85, Soc. Ital. di Fisica, Bologna) pp. 1–44.
- MCGARR, A. (1981), *Analysis of peak ground motion in terms of a model of inhomogeneous faulting*, J. Geophys. Res. 86, 3901–3912.
- MIKUMO, K. T. and MIYATAKE, T. (1978), *Dynamic rupture process on a 3D fault with nonuniform friction and near-field seismic waves*, Geophys. J. Roy. Astr. Soc. 54, 417–438.
- MORI, Y. and SHIMAZAKI, K. (1984), *High stress drops of short-period subevents from the 1968 Tokachi-Oki earthquake as observed on strong motion records*, Bull. Seismol. Soc. Amer. 74, 1529–1544.
- NUR, A. (1978), *Nonuniform friction as a physical basis for earthquake mechanics*, Pure Appl. Geophys. 116, 964–991.

- PAPAGEORGIOU, A. S. and AKI, K. (1983), *A specific barrier model for the quantitative description of inhomogeneous faulting and the prediction of strong ground motion. 1. Description of the model*, Bull. Seismol. Soc. Amer. 73, 953–978.
- PAPAGEORGIOU, A. S. and AKI, K. (1985), *Scaling law of far-field spectra based on observed parameters of the specific barriers model*, Pure Appl. Geophys. 123, 353–374.
- PURCARU, G. and BERCKHEMER, H. (1982), *Quantitative relations of seismic source parameters and a classification of earthquakes*, Tectonophysics 84, 57–128.
- SHEBALIN, N. V. (1971), *Comments on the dominant period, spectrum and source of large earthquakes*, in *The Problems of Engineering Seismology* (Nauka, Moscow) issue 15, pp. 50–78 (in Russian).
- SHTEINBERG, V. V., FREMD, V. M., and THEOPHILAKTOV, V. D. (1975), *Ground vibrations during large earthquakes on Kamchatka of 1971*, in *Large Kamchatka Earthquakes of 1971* (ed. S. A. Fedotov) (Vladivostok, Far East Sci. Center, Ac. Sci., USSR) pp. 7–14.
- SPUDICH, P. and CRANSWICK, E. (1984), *Direct observation of rupture propagation during the 1979 Imperial Valley earthquake using a short baseline accelerometer array*, Bull. Seismol. Soc. Amer. 74, 2083–2114.
- TRIFUNAC, M. D. and LEE, V. W. (1985), *Preliminary empirical model for scaling Fourier amplitude spectra of strong ground acceleration in terms of earthquake magnitude, source of station distance, site intensity and recording site conditions*, Rept. CE 85–03, Univ. of Southern California, 86 pp.

(Received August 3, 1987, revised March 18, 1988, accepted October 15, 1988)